Finite Element Investigation of Stationary Natural Convection of Light and Heavy Water in a Vessel Containing Heated Rods

Mohamed M. Mousa

Department of Basic Science, Benha Faculty of Engineering, Benha University, 13512, Egypt

Reprint requests to M. M. M.; E-mail: dr.eng.mmmm@gmail.com,
E-mail: mohamed.youssef@bhit.bu.edu.eg

Z. Naturforsch. **67a,** 421 – 427 (2012) / DOI: 10.5560/ZNA.2012-0040
Received December 14, 2011 / revised April 16, 2012

This numerical study investigates the steady state natural convection of light and heavy water entering a vessel from the left and leaving on the right. The cavity consists of a matrix of cylindrical heated rods as in light and heavy water reactors. The aim of the study is to describe the effects of water inlet velocity on the flow and thermal fields in presence of such heated obstacle. The investigations are conducted for different values of rods temperatures. From the numerical results, it is evident that the flow pattern and temperature fields are significantly dependent on the water inlet velocity and rods temperature.

Key words: Light Water; Heavy Water; Natural Convection; Heated Obstacle Galerkin Weighted Residual; Finite Element Method.

1. Introduction

The study of convective heat transfer and natural convection flow of light water (H_2O) and heavy water (D_2O) are of paramount importance in energy engineering. Various numerical and experimental methods have been proposed to examine characteristics of a flow inside cavities with and without obstacle because such geometries have realistic engineering and industrial applications, such as in the design of light and heavy water reactors, thermal design of building, air conditioning, cooling of electronic devices, chemical processing equipment, drying technologies etc. Many authors have studied natural convection in enclosures with partitions, fins, and blocks which influence the convection flow phenomenon. The effect of a centered heated square body on natural convection in a vertical enclosure was studied in [1]. The authors showed that heat transfer across the cavity is enhanced or reduced by a body with a thermal conductivity ratio less or greater than unity. The natural convective flow and heat transfer profiles for a heated cylinder placed in a square enclosure with various thermal boundary conditions are analyzed in [2]. In [3], the natural convection in a horizontal layer of fluid with a periodic array of square cylinder in the interior was studied. Authors of [4] investigated the stationary laminar natural convection in a square cavity filled with a fixed volume of conducting solid material consisting of either circular or square obstacles. In this article, the authors used a finite volume method and solved the governing equations. They found that the average Nusselt number for cylindrical rods was slightly lower than that for square rods. A numerical study of natural convection in a horizontal enclosure with a conducting body was considered in [5]. Natural convective heat transfer in square enclosures heated from below was investigated in [6]. The finite element method was used to analyze the natural convection flows in a square cavity with non-uniformly heated wall(s) in [7].

Recently, many authors have theoretically and experimentally investigated the flow, heat, and mass transfer in water and other different types of fluids as in the following investigations. Chen et al. [8] made an experimental study of air–water two-phase flow in an 8×8 rods bundle under pool condition for one-dimensional drift-flux analysis. Heo and Chung [9] have conducted an experimental investigation of natural convection heat transfer on the outer surface of inclined cylinders. Chae and Chung [10] have theoret-

ically and experimentally examined the effect of the pitch-to-diameter ratio on the natural convection heat transfer of two vertically aligned horizontal cylinders In [11], Laguerre et al. have conducted an experimental and numerical study of heat and moisture transfers by natural convection in a cavity filled with solid obstacles. Persoons et al. [12] have discussed the close interaction between local fluid dynamics and natural convection heat transfer from a pair of isothermally heated horizontal cylinders submerged in water. Natural convection heat transfer of nanofluids in annular spaces between long horizontal concentric cylinders maintained at different uniform temperatures was investigated theoretically in [13] by Cianfrini et al. An analytical and numerical study of natural convection in a shallow rectangular cavity filled with nanofluids have been reported in [14] by Alloui et al. In [15], Atayılmaz has experimentally and numerically examined the natural convection heat transfer from horizontal concentric cylinders.

Comparatively little articles have been reported on natural convection of heavy water in a vessel. The present study addresses the effects water inlet velocity and obstacles temperature which may increase or decrease the heat transfer on natural convection in a vessel with heated circular solid rods. From the obtained numerical results, it can be noted that the heat transfer in D_2O is less than that in H_2O. Numerical solutions are obtained using the Galerkin weighted residual finite element method [16 – 19]. The numerical results are presented graphically in terms of surface and curves at certain positions for different values of water inlet velocity and rods temperatures.

2. Problem Formulation

Consider an array of heated rods submerged in a vessel with H_2O or D_2O entering from left and leaving on right as shown in Figure 1.

The problem is formulated in the two-dimensional (2D) domain because of neglecting any end effects from the vessel walls. Therefore, the solution is constant in the direction of the heating tubes and there are no variations in the third dimension. In order to decrease computation time and complexity, the symmetry of the system can be used. So, the system can be described using two sections of the heated rods array (indicated by the dashed lines in Fig. 1) as shown in Figure 2.

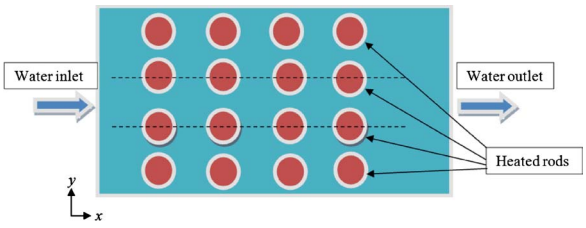

Fig. 1 (colour online). Schematic diagram of the problem (view from top).

Fig. 2 (colour online). Computational domain of the problem.

Table 1. Characteristics of light water and heavy water.

Quantity [dimension]	Symbol	Light water (H_2O)	Heavy water (D_2O)
Density $[kg/m^3]$	ρ	1000	1105
Dynamic viscosity $[Pa \cdot s]$	μ	0.001	0.00125
Heat capacity $[J/(kg \cdot K)]$	C_p	4200	4220
Thermal conductivity $[W/(m \cdot K)]$	k	0.6	0.45

The computational domain is considered as $0 \leq x \leq 1$, $0 \leq y \leq 0.2$, and the radius of a circular rod is 0.5. All dimensions are given in meters. The centers of the heated rods are located at $x = 0.15$, 0.35, 0.55, and 0.75. The distance between any two adjacent rods in y-direction is 0.1. The water enters the vessel at constant temperature $T_{in} = 293$ K and constant normal velocity v_{in}. The uniform temperature of the rods is assumed to be T_{heat}. Here T_{in} is much less than T_{heat}. There is no viscose stress at all the free boundaries and the pressure is considered to be zero there. The rods are consider as walls without slip. The characteristics of H_2O and D_2O used in the computations are listed in Table 1.

3. Mathematical Formulation

In the current problem, we have considered that the water flow is a steady-laminar one. The gravitational force and radiation effect are neglected here. The incompressible Navier–Stokes equations with a heat transfer equation are the best model for this problem. So, the problem governing equations can be written as

follows:

$$\frac{\partial u}{\partial x}+\frac{\partial v}{\partial y}=0\,, \tag{1}$$

$$\rho\left(u\frac{\partial u}{\partial x}+v\frac{\partial u}{\partial y}\right)=-\frac{\partial p}{\partial x}+\mu\left(\frac{\partial^2 u}{\partial x^2}+\frac{\partial^2 u}{\partial y^2}\right), \tag{2}$$

$$\rho\left(u\frac{\partial v}{\partial x}+v\frac{\partial v}{\partial y}\right)=-\frac{\partial p}{\partial y}+\mu\left(\frac{\partial^2 v}{\partial x^2}+\frac{\partial^2 v}{\partial y^2}\right), \tag{3}$$

$$\rho C_p\left(u\frac{\partial T}{\partial x}+v\frac{\partial T}{\partial y}\right)=k\left(\frac{\partial^2 T}{\partial x^2}+\frac{\partial^2 T}{\partial y^2}\right), \tag{4}$$

where u and v are the velocities in the x and y-directions, respectively. T is the temperature and p is the pressure. The boundary conditions are

$$\begin{aligned}&u(0,y)=v_{\text{in}}\,,\ \ T(0,y)=T_{\text{in}}\,,\\ &u_x(1,y)=0\,,\ \ v(0,y)=0\,,\ \ v_x(1,y)=0\,,\\ &u_y(x,0)=u_y(x,0.2)=v_y(x,0)=v_y(x,0.2)=0\,.\end{aligned}$$

At the heated rod surface $u(x,y)=v(x,y)=0$ and $T(x,y)=T_{\text{heat}}$.

4. Methodology

The numerical technique which has been used to solve the model equations (1)–(4) subject to the given boundary conditions is the finite element formulation based on the Galerkin weighted residual method. The applications of this method are well described in [16–19]. Based on the considered method, the global solution domain is discretized into a number of suitable finite elements as a grid, which are composed of non-uniform triangular elements using commercially available grid generators such as ANSYS. Figure 3 shows the mapping of the given domain by triangle elements as an unstructured mesh.

Based on the Galerkin weighted residual method, the unknown functions u, v, and T in (1)–(4) within each element are approximated by using interpolation functions constructed as the products of linear Lagrangian interpolation functions in x and y-directions:

$$\begin{aligned}&u\approx\tilde{u}=\sum_{i=1}^{3}N_i(x,y)\cdot u_i\,,\ \ v\approx\tilde{v}=\sum_{i=1}^{3}N_i(x,y)\cdot v_i\,,\\ &T\approx\tilde{T}=\sum_{i=1}^{3}N_i(x,y)\cdot T_i\,,\end{aligned} \tag{5}$$

where $N_i(x,y)$ are the interpolation functions associated with nodes $i=1,2,3$ for each element in the unstructured mesh. Therefore these elements are said to be three-node bilinear tensor product elements. The weighted residual statement of the problem thus transforms the governing equations (1)–(4) into a system of integral equations. As an example, the integral equation associated with (1) can be written as

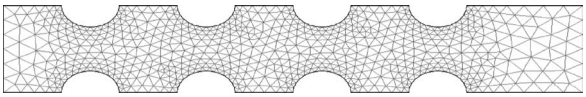

Fig. 3. Unstructured mesh for the problem domain.

$$\iint_{\Omega e} w_j\left(\frac{\partial\tilde{u}}{\partial x}+\frac{\partial\tilde{v}}{\partial y}\right)\mathrm{d}x\,\mathrm{d}y=0\,,\ \ j=1,2,3\,, \tag{6}$$

where Ωe is the domain of an element e, and w_j are linearly independent weight functions. In the standard Galerkin method, weight functions are identical to the element shape functions and hence

$$\iint_{A}[N]^{\mathrm{T}}\left(\frac{\partial\tilde{u}}{\partial x}+\frac{\partial\tilde{v}}{\partial y}\right)\mathrm{d}A=0\,. \tag{7}$$

We have used the Gauss quadrature method in order to perform the integration involved in each term of the integral equations. Then a system of nonlinear algebraic equations is obtained. Boundary conditions are incorporated into the assembled global system of equations to make it determinate. Now, the modified nonlinear system of algebraic equations is converted into linear algebraic equations using Newton's method. Finally, the obtained system of linear equations, which represents the unknowns at each node of the triangular elements across the solution domain is solved using the triangular factorization method. An error analysis was made in order to estimate the number of iterations needed for convergence.

5. Results and Discussion

Present finite element representation is applied to simulate the steady natural convection of light and heavy water in a cavity consisting of a matrix of cylindrical heated obstacles. Effects of parameters such as normal inlet velocity and heated obstacle temperature on water temperature and velocity field inside the cavity have been studied. The results have been presented

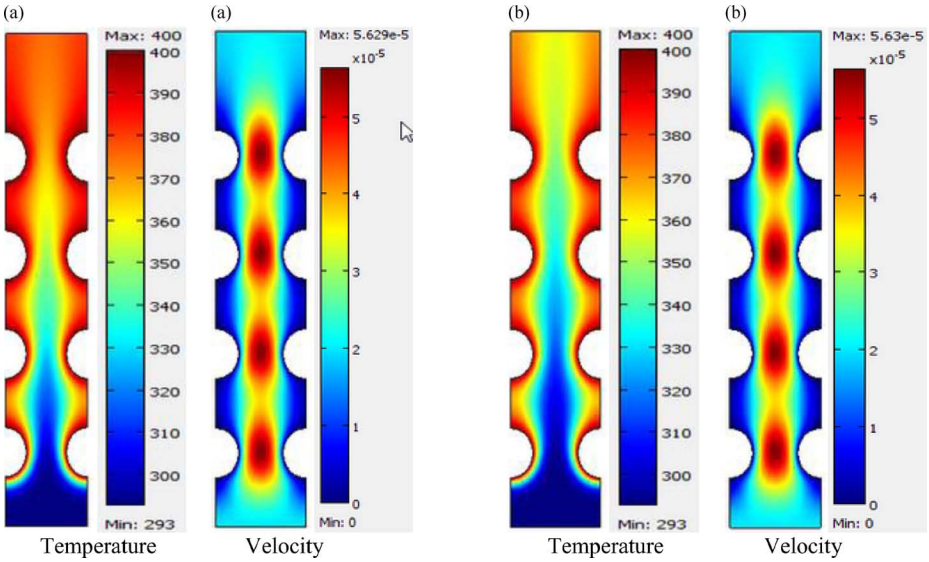

Fig. 4 (colour online). Temperature and velocity profiles for (a) H_2O and (b) D_2O when $v_{in} = 2 \cdot 10^{-5}$ m/s and $T_{heat} = 400$ K.

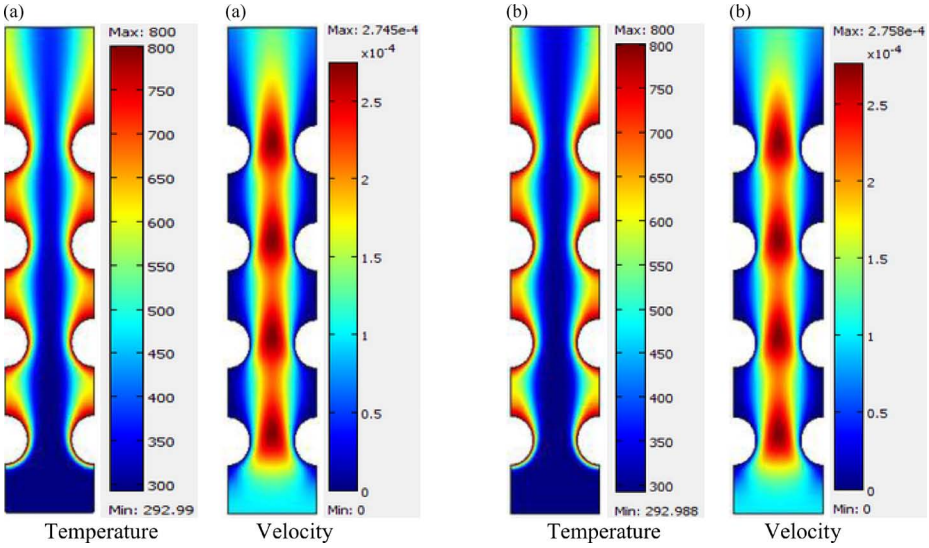

Fig. 5 (colour online). Temperature and velocity profiles for (a) H_2O and (b) D_2O when $v_{in} = 0.0001$ m/s and $T_{heat} = 800$ K.

in two categories. The first category illustrates the difference between heat transfer in light and heavy water at the same inlet velocity and obstacle temperature by presenting the solution domain in a 2D plot. In this type of presentation, the difference between heat transfer in same water at different obstacles temperature and the difference between velocity fields in same water at different inlet velocities can be illustrated. The second category illustrates the influence of the inlet velocity and temperature of the heated cylinders on fluid temperature and velocity by presenting the results in a 1D plot. In the 2D representation, a surface plot represents the temperature [K] and the velocity field [m/s].

A comparison between the influences of inlet velocity and obstacle temperature on the water velocity field as well as natural convection has been demonstrated in Figures 4 – 6. Moreover, a comparison between the natural convection in light and heavy water at the same v_{in} and T_{heat} can also be seen from these figures. From Figure 4a, it can be noticed that the H_2O temperature at the outlet reaches the boiling temperature, however

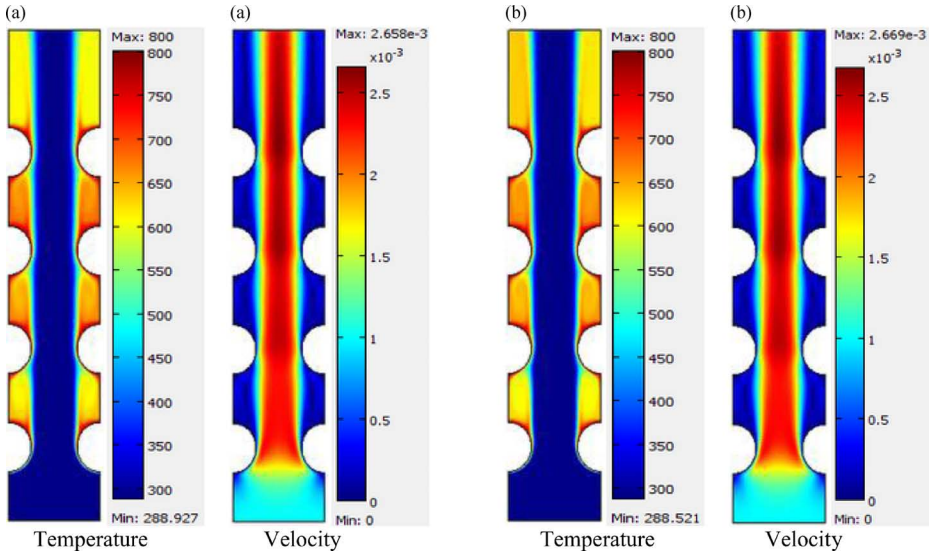

Fig. 6 (colour online). Temperature and velocity profiles for (a) H_2O and (b) D_2O when $v_{in} = 0.001\,m/s$ and $T_{heat} = 800\,K$.

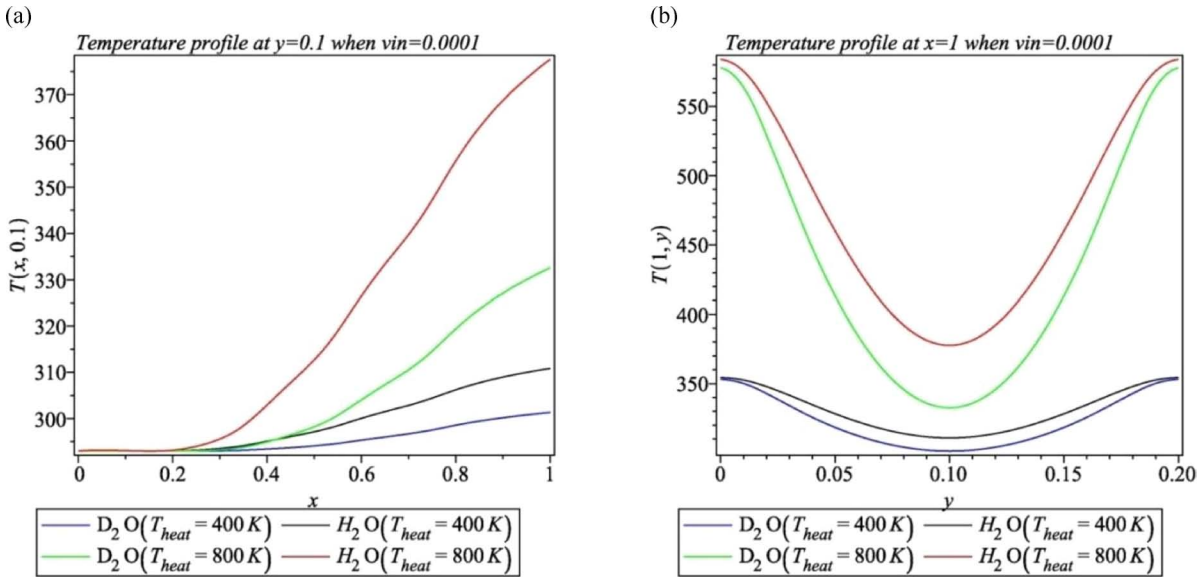

Fig. 7 (colour online). Comparison between temperature profiles for H_2O and D_2O when $v_{in} = 0.0001\,m/s$ and various T_{heat}: (a) at $y = 0.1$, i.e. $T(x, 0.1)$; (b) at $x = 1$, i.e. $T(1, y)$.

in case of D_2O, the temperature at the outlet doesn't reach the boiling temperature at the same conditions as shown in Figure 4b. Therefore, we can conclude that the convection in D_2O is less than that in H_2O. This conclusion can be drawn by comparing the temperature profiles in Figure 5a with Figure 5b and in Figure 6a with Figure 6b. From the previous conclusion and the fact that the heavy water absorbs fewer neutrons than light water, the scientists prefer using the heavy water as a coolant and moderator in nuclear reactors instead of H_2O. A second result which can be drawn from Figures 4 – 6 is that as the inlet velocity v_{in} increases the convection decreases. As third result can be noticed that the behaviour of the water velocity field is majorly influenced by v_{in} and slightly by the properties of water.

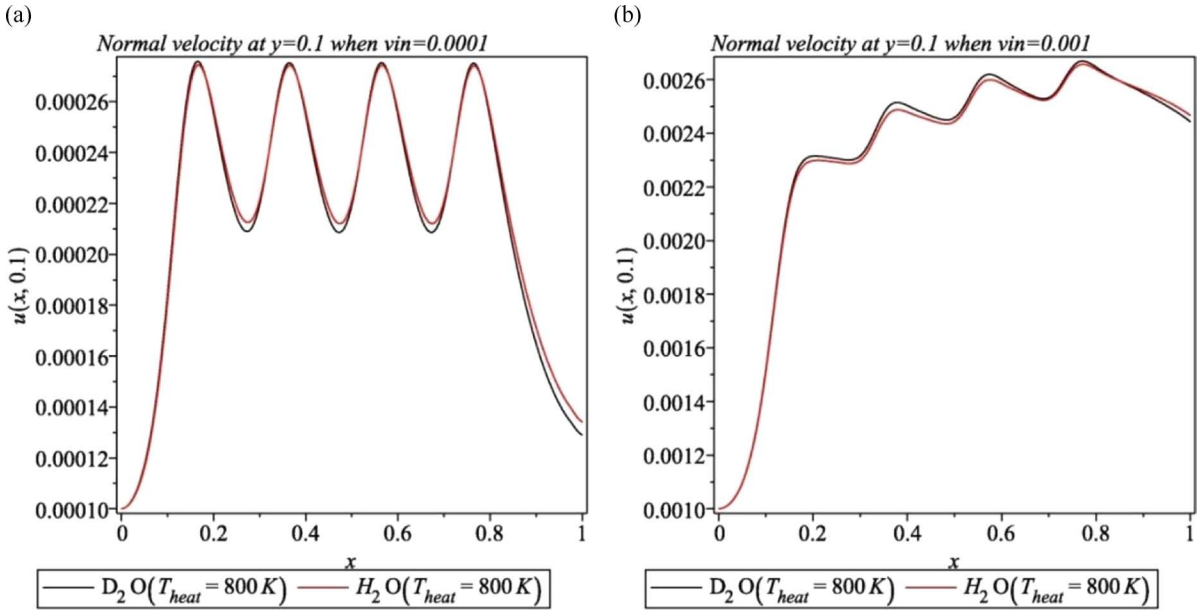

Fig. 8 (colour online). Comparison between velocity field $u(x, 0.1)$ for H_2O and D_2O when $T_{\text{heat}} = 800$ K and various v_{in}: (a) $v_{\text{in}} = 0.0001$ m/s; (b) $v_{\text{in}} = 0.001$ m/s.

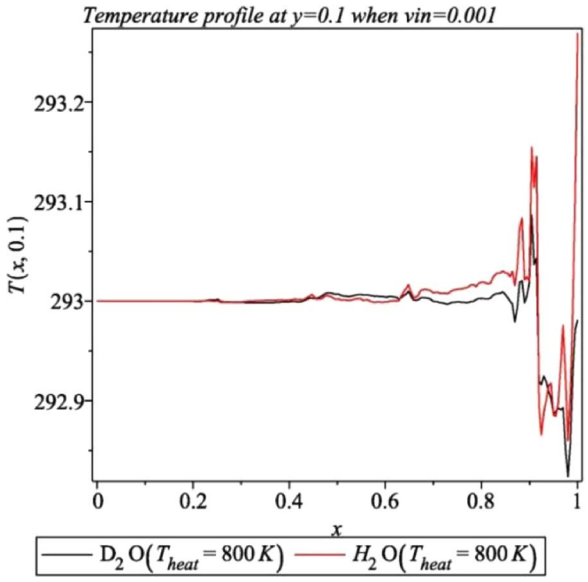

Fig. 9 (colour online). Temperature profile $T(x, 0.1)$ for H_2O and D_2O when $v_{\text{in}} = 0.001$ m/s and $T_{\text{heat}} = 800$ K.

All the previous discussed results can be deduced by examining the results shown in Figures 7 and 8. The new results which can be drawn from the 1D representation are shown in Figure 9 and can be summarized in that for both H_2O, D_2O and in case of relatively high inlet velocity v_{in}, say 0.001 m/s, the difference between temperature of the inlet water and outlet water at the symmetry axis ($y = 0.1$) is very small even for very high rods temperature T_{heat}. Hence, the increasing in the water inlet velocity will decrease the water natural convection.

6. Conclusion

A numerical analysis of natural convection in both light and heavy water in vessel containing heated cylindrical obstacles has been carried out. The finite element formulation based on the Galerkin weighted residual method is used to simulate the present model. The main conclusions which can be drawn from the obtained results are as follows:

1) The natural convection in heavy water is less than that in light water at the same conditions.
2) Heavy water is the optimal choice for cooling fuel rods in nuclear reactors.
3) The influence of water inlet velocity on convection and velocity field is remarkable.
4) The water velocity field is extremely influenced by v_{in} and slightly by the type of water.
5) All the presented results are consistent with thermodynamic physics.

[1] J. M. House, C. Beckermann, and T. F. Smith, Numer. Heat Transfer A **18**, 213 (1990).
[2] D. G. Roychowdhury, S. K. Das, and T. S. Sundararajan, Heat Mass Transfer **38**, 565 (2002).
[3] M. Y. Ha, H. S. Yoon, K. S. Yoon, S. Balachandar, I. Kim, J. R. Lee, and H. H. Chun, Numer. Heat Transfer A **41**, 183 (2002).
[4] E. J. Braga and M. J. S. de Lemos, Int. Commun. Heat Mass Transfer **32**, 1289 (2005).
[5] J. R. Lee and M. Y. Ha, Int. J. Heat Mass Tran. **48**, 3308 (2005).
[6] B. Calcagni, F. Marsili, and M. Paroncini, Appl. Therm. Eng. **25**, 2522 (2005).
[7] S. Roy and T. Basak, Int. J. Eng. Sci. **43**, 668 (2005).
[8] S.-W. Chen, Y. Liu, T. Hibiki, M. Ishii, Y. Yoshida, I. Kinoshita, M. Murase, and K. Mishima, Int. J. Heat Fluid Fl. **33**, 168 (2012).
[9] J.-H. Heo and B.-J. Chung, Chem. Eng. Sci. **73**, 366 (2012).
[10] M.-S. Chae and B.-J. Chung, Chem. Eng. Sci. **66**, 5321 (2011).
[11] O. Laguerre, S. Benamara, D. Remy, and D. Flick, Int. J. Heat Mass Tran. **52**, 5691 (2009).
[12] T. Persoons, I. M. O'Gorman, D. B. Donoghue, G. Byrne, and D. B. Murray, Int. J. Heat Mass Tran. **54**, 5163 (2011).
[13] M. Cianfrini, M. Corcione, and A. Quintino, Appl. Therm. Eng. **31**, 4055 (2011).
[14] Z. Alloui, P. Vasseur, and M. Reggio, Int. J. Therm. Sci. **50**, 385 (2011).
[15] S. Ö. Atayılmaz, Int. J. Therm. Sci. **50**, 1472 (2011).
[16] S. Parvin and R. Nasrin, Nonlin. Anal. Model. Control **16**, 89 (2011).
[17] C. Taylor and P. Hood, Comput. Fluids **1**, 73 (1973).
[18] P. Dechaumphai, Finite Element Method in Engineering, 2nd edn., Chulalongkorn University Press, Bangkok 1999.
[19] V. Nassehi and M. Parvazinia, Finite Element Method in Engineering, Imperial College Press, London 2010.

Erratum

G. Furman and S. Goren, Dipolar Order and Spin-Lattice Relaxation in a Liquid Entrapped into Nanosize Cavities, Z. Naturforsch. **66a**, 779 (2011).

Reprint requests should be done to G. F.; E-mail: gregoryf@bgu.ac.il

The calculated density matrix (14) was in error. Therefore, the following changes should be made:

1. Change (14) to

$$\rho(\tau) = 1 - \beta_1 \omega_0 \sum_{\kappa} \left[I_\kappa^y \cos\left(\frac{3\tau G}{4} \left(I_z - I_\kappa^z \right) \right) - I_\kappa^x \sin\left(\frac{3\tau G}{4} \left(I_z - I_\kappa^z \right) \right) \right]. \tag{14}$$

2. Change (15) to

$$\rho_2 = \left\{ 1 - \beta_1 \omega_0 \sum_{\kappa} \left[I_\kappa^y \cos \Phi_\kappa - \left(I_\kappa^x \cos\xi - I_\kappa^z \sin\xi \right) \sin \Phi_\kappa \right] \right\}, \tag{15}$$

   where $\Phi_\kappa = \left\{ \frac{3\tau G}{4} \left[\left(I_z - I_\kappa^z \right) \cos\xi + \left(I_x - I_\kappa^x \right) \sin\xi \right] \right\}$.
3. Change (17) to

$$\beta_d = -\frac{\mathrm{Tr}\{\rho_2 \bar{H}_d\}}{\mathrm{Tr}\{\bar{H}_d^2\}} = \frac{3}{4} G \frac{1}{\omega_{\mathrm{loc}}^2} \sin(2\xi) \frac{\mathrm{Tr}\{\rho(\tau) \sum_{\mu \neq \eta} \left(I_\mu^z I_\eta^x + I_\eta^z I_\mu^x \right)\}}{\mathrm{Tr} I_z^2}. \tag{17}$$

4. In the last sentence of Sect. 3, delete "and $\tau = \frac{2}{3} \frac{\pi}{G}$".
5. Change the second sentence of Sect. 5 to:
   It can be seen from (26) that the spin-lattice relaxation time T_{1d} depend on the cavity size V, its shape F and orientation θ, $T_{1d} \sim \left(\frac{V}{F(1-3\cos^2\theta)} \right)^2$.
6. Delete the third sentence of Sect. 5.

We thank Professor J. Jeener for pointing out this error.